The Journal of the Korean Society of
Coastal and Ocean Engineers
Vol. 5, No. 2, pp. 151~171, June 1993

A Review of Tidal Models for the East China and Yellow Seas
東中國海와 黃海의 潮汐數値模型에 關한 過去의 硏究

Byung Ho Choi* and Guohong Fang**
崔秉昊* · 方國洪**

Abstract □ The review presented herein covers most of previous works on tidal models of the East China Sea and the Yellow Sea performed over past two decades including some earlier efforts. General description of tides in the region is given based on both numerically derived tidal charts, current ellipses and intelligently drawn empirical tidal charts. Some aspects of bottom tidal dissipation, tidal mixing, tidal sedimentation and tidal circulation utilizing the numerical tidal models are presented, and further discussions on inherent problems and development of the models are also given.

要 旨 : 本 綜說에서는 過去 20年에 걸친 東中國海와 黃海의 潮汐數値模型에 대해 槪觀하였다. 潮汐模型 및 經驗的인 潮汐圖에 依據하여 이 海域의 潮汐樣相에 대해 敍述하였으며 이와 關聯된 海底潮汐消散, 潮汐混合, 堆積 및 循環에 대하여 記述하였다. 또한 潮汐模型에 關聯된 問題點과 改善方法에 대하여 論議하였다.

1. INTRODUCTION

Freshwater input from rivers, surface wind, solar radiation, surface cooling, and external water masses all play important roles in determining the patterns of water characteristics and currents in the Yellow Sea and the East China Sea continental shelf, but the region is most remarkable for the large tides along the west coast of Korea, Chinese coast, and for the complexity of tidal phenomena.

The first tidal chart for the region was presented by Harris (1897) in U.S. Coast and Geodetic Survey (Fig. 1). In this diagram general propagation patterns of semidiurnal tides are well shown although two amphidromies in the Liaodong and off Jiangsu (western Yellow Sea) are missing.

During the late 1920's and early 1930's extensive studies of this shelf sea area were reported and a considerable number of tidal measurements were made, from which co-tidal and co-range charts of diurnal and semidiurnal tides were drawn (Fig. 2). These charts prepared by Ogura Sinkiti of Japanese

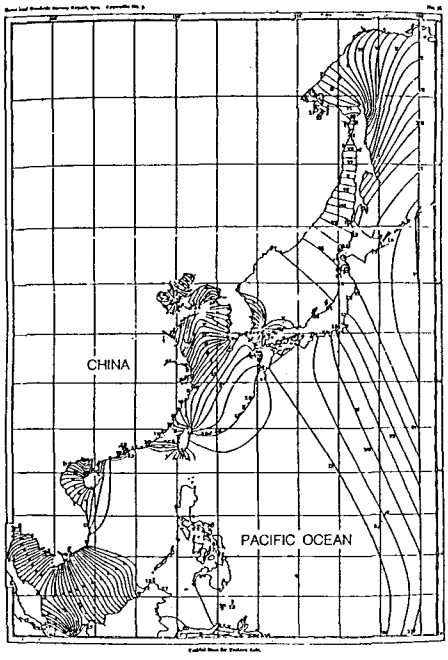

Fig. 1. Cotidal lines for the Eastern Asia (Harris 1897).

*韓國 成均館大學校 土木工學科 (Department of Civil Engineering, Sung Kyun Kwan University, Suwon, Korea)
**中國 科學院 海洋硏究所 (Institute of Oceanology, Academia Sinica, Qingdao, China)

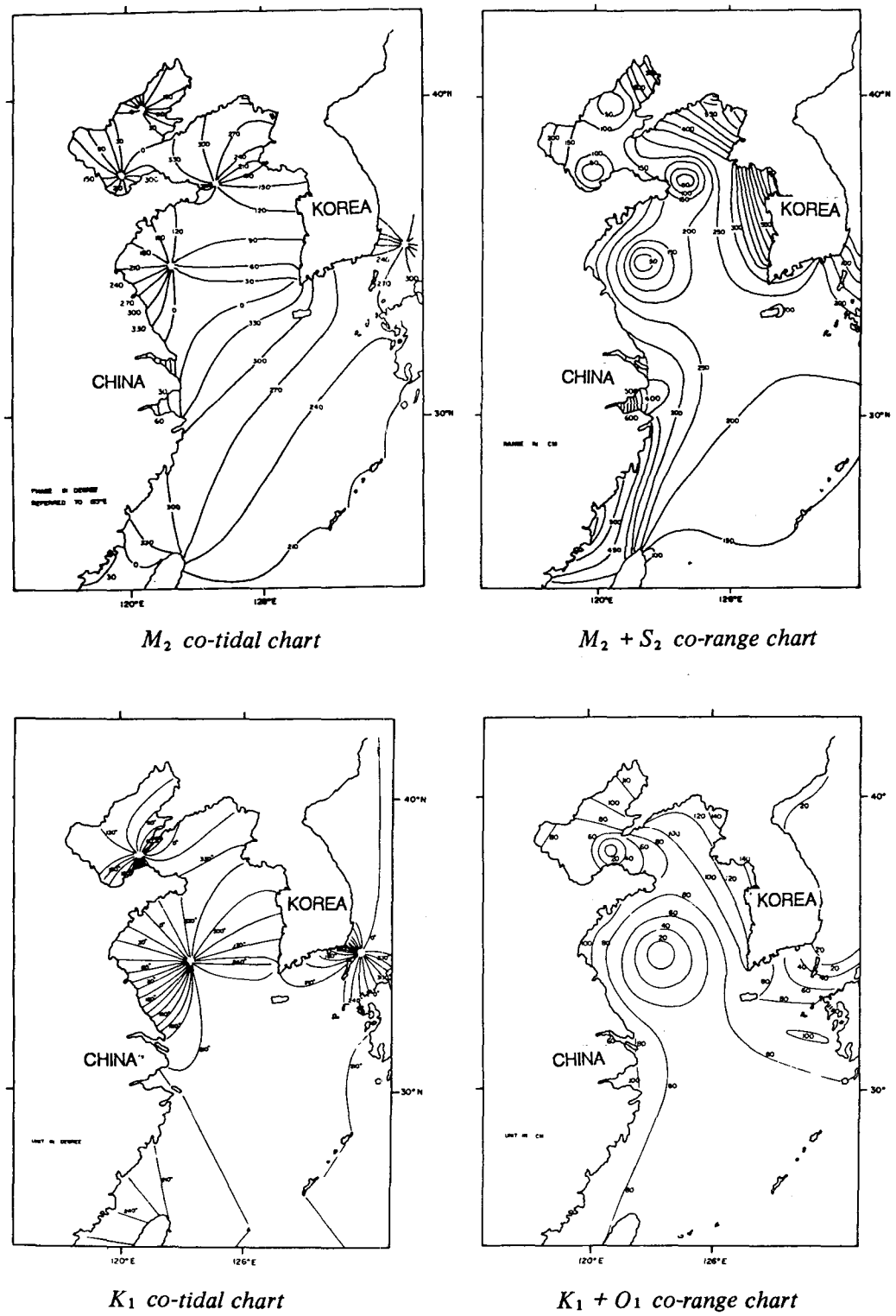

M_2 *co-tidal chart* $M_2 + S_2$ *co-range chart*

K_1 *co-tidal chart* $K_1 + O_1$ *co-range chart*

Fig. 2. Tidal charts of diurnal and semidiurnal tide in the Yellow sea (Ogura, 1933).

existing coamplitude charts of M2, S2, K1 and O1 tides taken from Nishida, hydrographic department of Japan, Maritime Safety Agency. units in cm. charts are drawn empirically based on coastal observations.

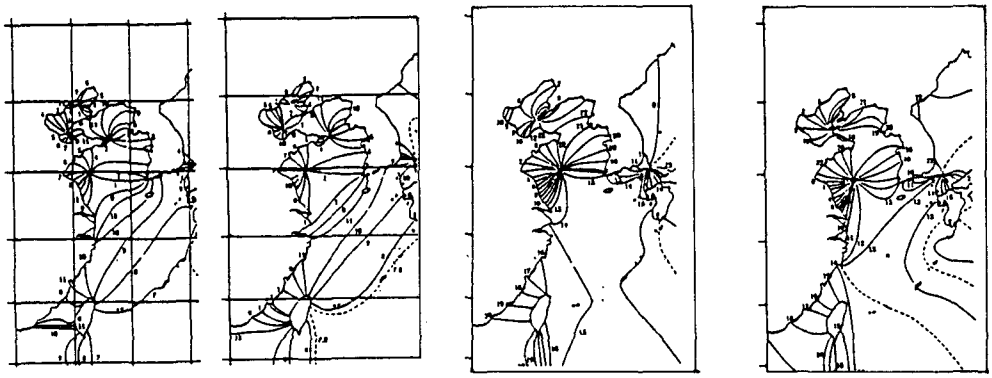

existing cotidal charts of M2, S2, K1 and O1 tides taken from Nishida, hydrographic department of Japan, Maritime Safety Agency. refernce time is taken as -9 hours. charts are drawn empirically based on coastal observations.

Fig. 3. Coamplitude and cotidal charts of the M_2, S_2, K_1, O_1 tide (Nishida, 1980).

Hydrographic Department have been used as standard tidal charts for several decades. Nishida (1980) has redrawn the map for the Western North Pacific for separate four (M_2, S_2, K_1, O_1) constituents but general tidal patterns were identical with previous chart in the East China Sea region (Fig. 3). Fang (1986) also presented tidal charts for the Yellow Sea and the East China Sea (Fig. 4) based on the method similar to Proudman and Doodson (1924) but also adopted numerical results combined with coastal observations (Fang, 1985).

Russian scientists (Boris, 1958; Tsiklauri and Boris, 1961; Stepanov and Boris, 1964) reported the first application of two-dimensional mathematical models on the one hand to the Yellow Sea and on the other hand, to the Gulfs of Bohai and Liaodong, employing boundary-value methods which call for much tidal data at external boundary points along the coast and open boundary. While the latter models were satisfactorily used to reproduce the M_2 and K_1 tides in the Gulf of Liaodong and Bohai where extensive tidal data exists, the Yellow Sea model was only used to test the sensitivity of the tides of that area to changes in the boundary tidal input data, depths along the boundaries and Coriolis parameter. Their results indicated that the com-

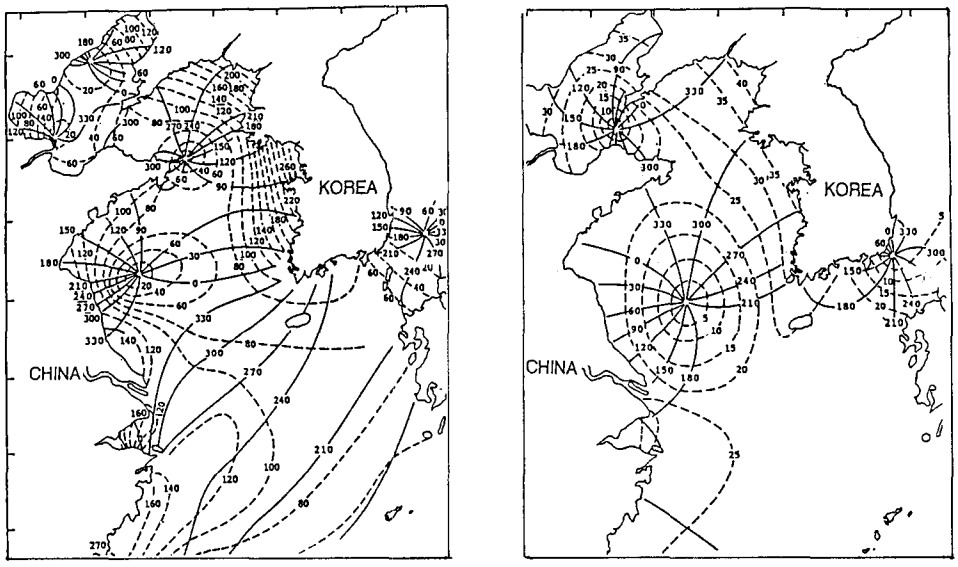

M2 tidal chart from the numerical model of Fang, ASIO, China.
Unit of amplitude (dotted line) in centimeters and unit of phase lag in degree referred to 120 deg East Longitude.

K1 tidal chart from the numerical model of Fang, ASIO, China.

Fig. 4. Tidal charts of M_2, K_1 tides (Fang, 1986).

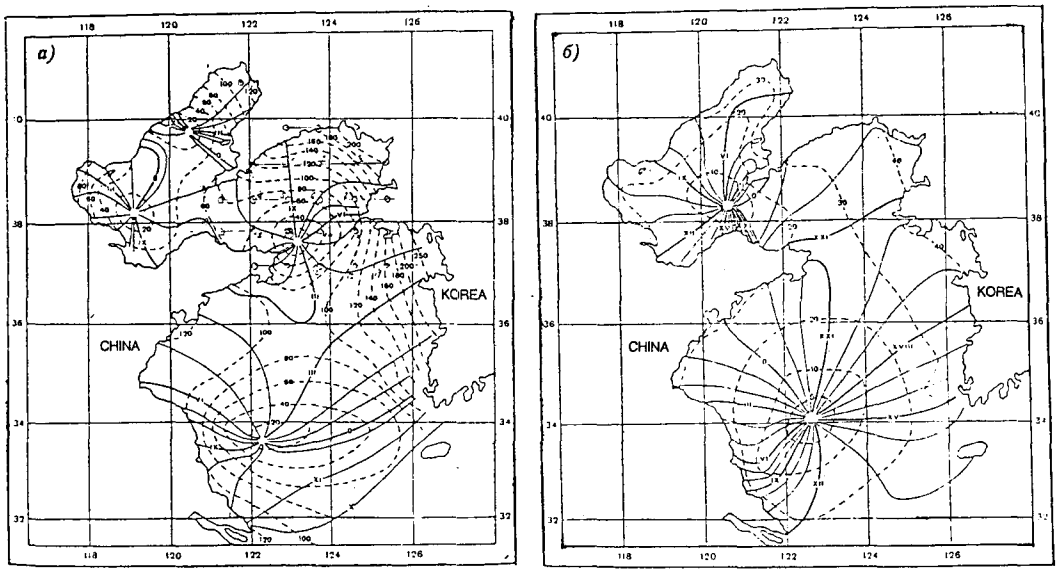

Fig. 5. Computed tidal charts (Boris, 1958).

puted tides in the Yellow Sea (Fig. 5) were highly sensitive to even small changes in levelling data and the depths along the boundaries.

During last two decades series of numerical tidal models have been reported by Chinese, Japanese and Korean scientists and it was demonstrated by these models that tides can be satisfactorily reproduced thus providing general information on the tidal dynamics in this region. In this review numerically computed tidal charts from published sources

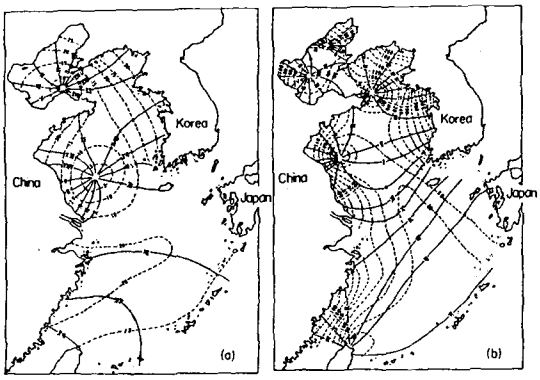

Fig. 6. Computed tidal charts (Shen, 1981).

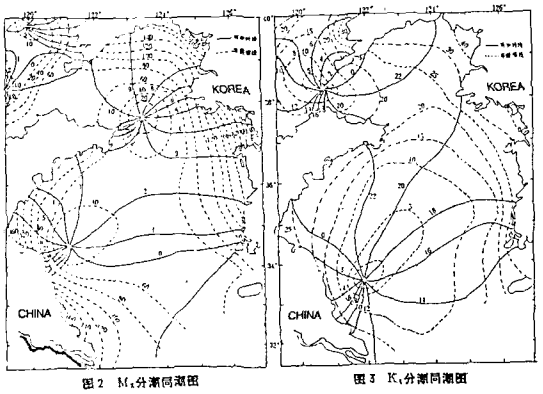

Fig. 7. Computed tidal charts (Liu *et al.*, 1983).

are collected and compared with intelligently drawn empirical tidal charts and tidal observations.

2. TIDAL CHARTS AND TIDAL MODELS

Numerical simulations of tides in the Yellow Sea were conducted by many Chinese authors since 1970. The co-tidal charts of principle constituents M_2, S_2, K_1 and O_1 for the East China Sea (Fig. 6) were presented on numerical solution by boundary value method (Shen, 1981). Several works concerning the tidal problems in the Bohai Sea have been done. For example, the tide-induced residual current (Dou *et al.*, 1981) and the shallow-water tide M_4 in the Bohai Sea were given (Sun *et al.*, 1981). The tides and tidal currents in the Jiaozhou Bay were studied in some detail (Wang *et al.*, 1980). Some of the computations are related to the studies of pollutants dispersion (Dou *et al.*, 1981, Wang *et al.*, 1980). Liu *et al.* (1983) presented M_2 and K_1 tidal distributions of the Yellow Sea (Fig. 7) based on the numerical computation in combination with the observation. Xia and Wang (1984) also presented M_2 and K_1 tidal distributions of the Yellow Sea (Fig. 8). Fang (1985) used finite difference-least square technique to solve the overdetermined problem formed from incorporation of boundary conditions and empirical data into a single model and M_2 tidal distribution was presented (Fig. 9). Zhang *et al.* (1991) at Hohai University developed a two-dimensional tide and surge model for the Yellow Sea and the East China Sea. The model has similar

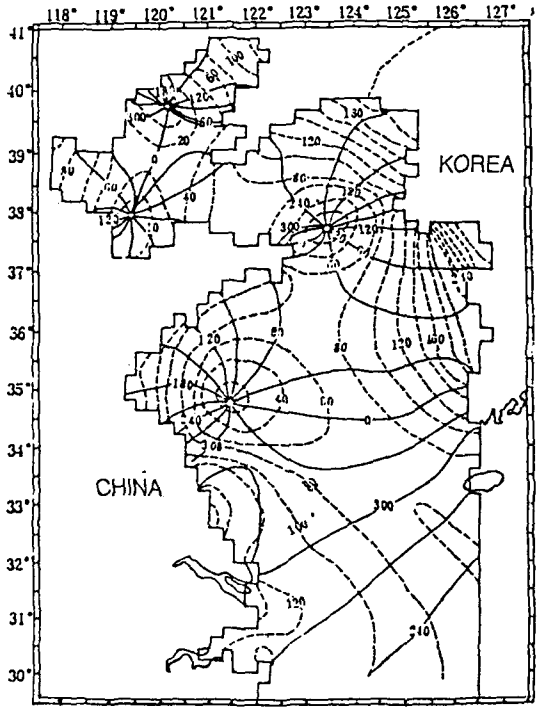

图 2 M_2分潮等潮图

图例：……等振幅线，——等潮时线。

Fig. 8. Computed tidal charts (Xia and Wang, 1984).

open boundary to that of Japanes Hydrographic Department and grid solution is about 20Km covering the whole shelf including two times of 1:3 mesh refinement focussing on Sanman Bay (Fig. 10). The model incorporated 6 tidal constituents at open boundary and was used to compute typhoon

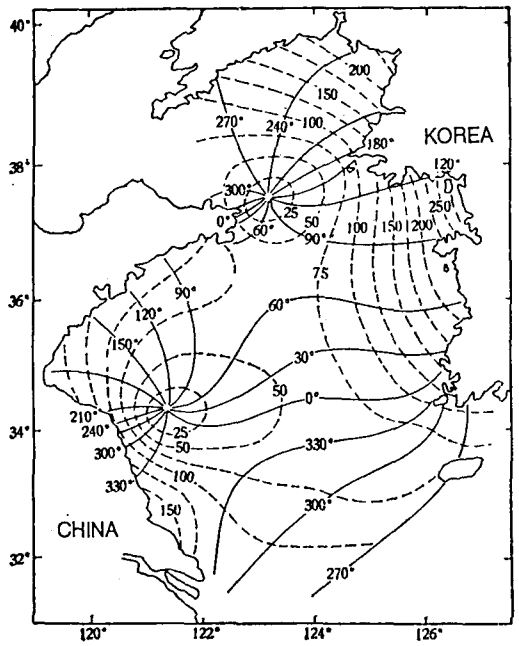

Fig. 9. Computed tidal charts (Fang, 1986).

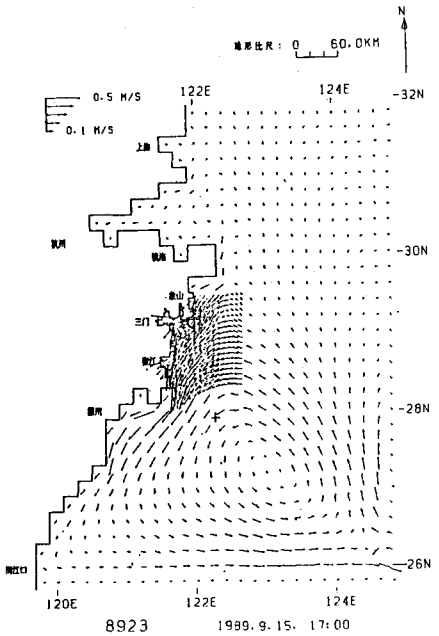

Fig. 11. Computed tide and current fields (Zhang *et al.*, 1991).

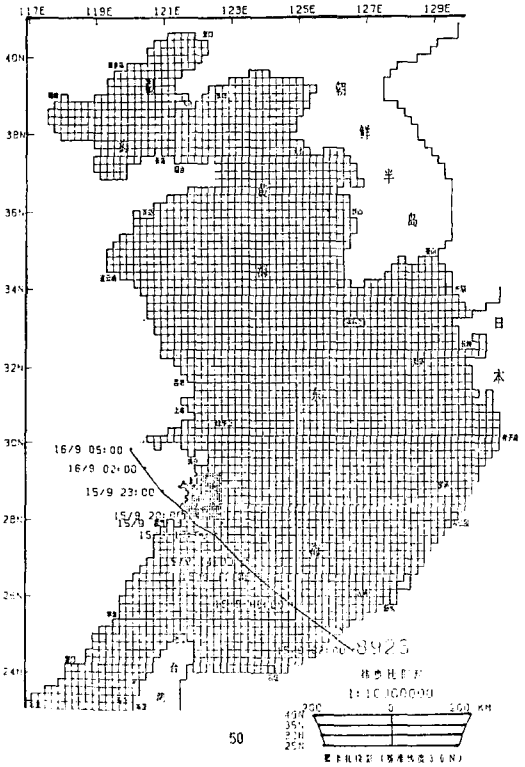

Fig. 10. Model grids for tide and surge computation (Zhang *et al.*, 1991).

surge of september 1989 for safety evaluation of coastal nuclear power plant (Fig. 11).

Numerical modelling efforts for predicting tidal changes due to coastal development in the eastern Yellow Sea was first imputus for dynamic modelling in the region. The initial models were developed at KORDI with the assistance from Bidston Observatory, IOS (now Proudman Oceanographic Laboratory). A series of tidal models of KORDI (Choi, 1980, Yum, 1978, An, 1977, Kang *et al.*, 1991) has been established over the entire continental shelf as well as concentrating on the Yellow Sea basin. General information on the tidal dynamics in the region has been provided via these models. Verification of the shelf model has been performed by coastal observations and US-China cooperative measurements. There was genernal agreement between the observation and the model results (Choi, 1980; Larsen *et al.*, 1985) which supports the assumed boundary conditions and numerical procedures. Fig. 12 shows model-derived tidal charts. In the principal axes of M_2 tidal ellipses charts shown (Fig. 13) gives an overall impression of the magnitude and direction of M_2 tidal current distribution repre-

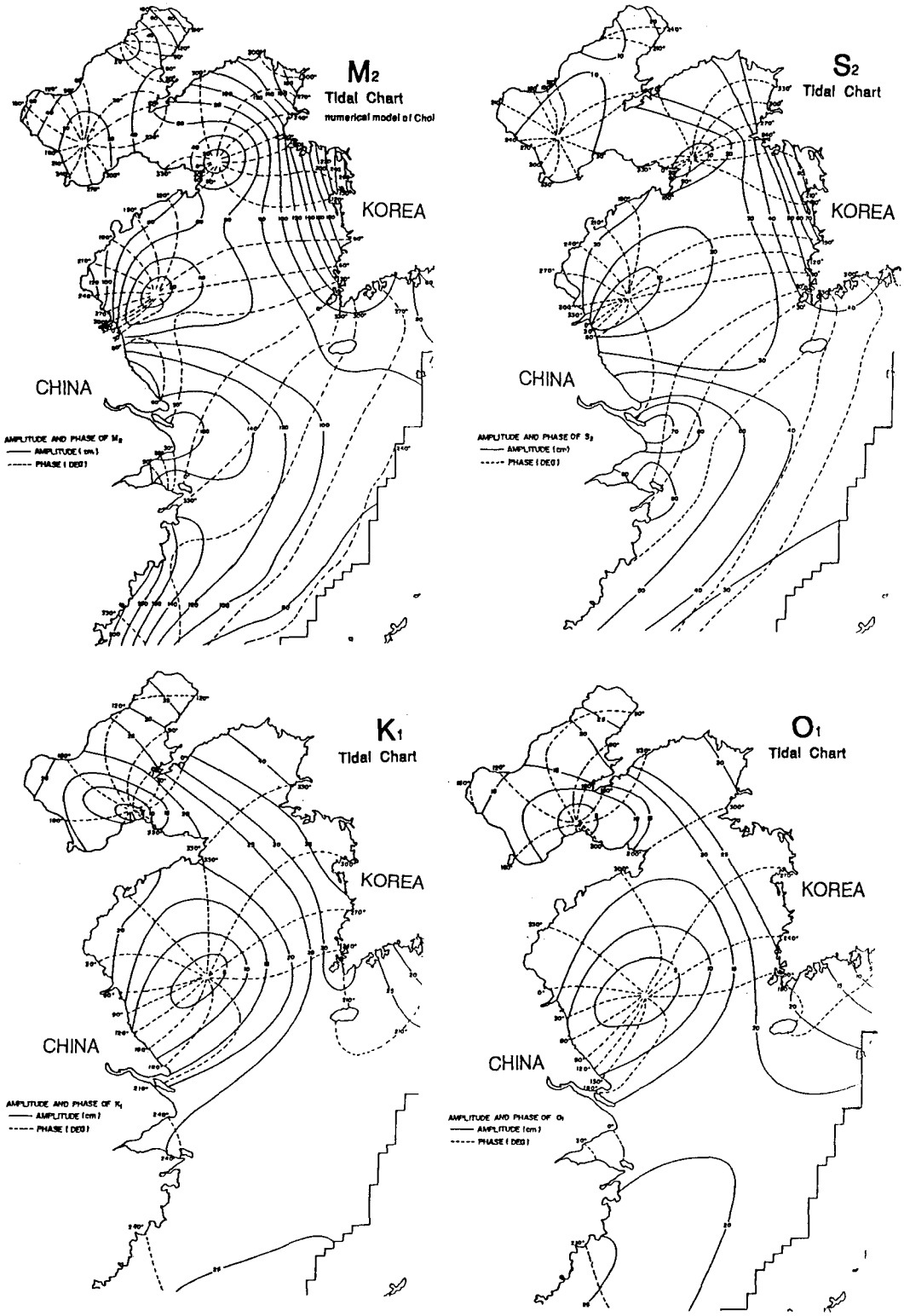

Fig. 12. Computed tidal charts (Choi, 1980).

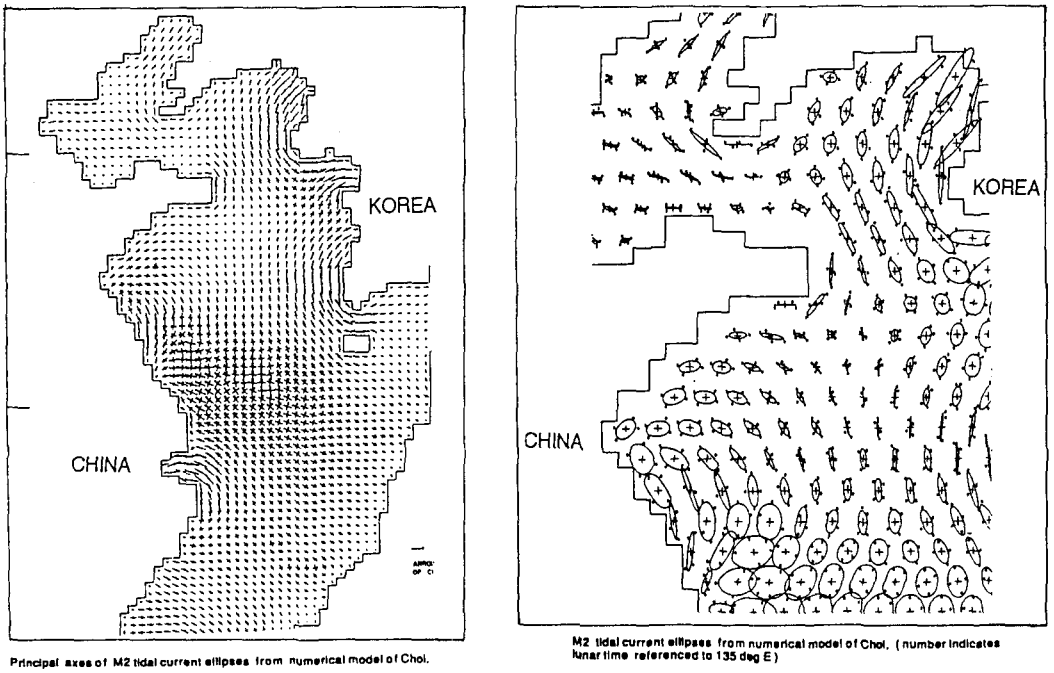

Fig. 13. Comuted M_2 tidal current ellipse (Choi, 1980).

senting the maximum and minimum velocities as major and minor axes respectively. Tide and surge models covering different regions are established at KORDI, SNU (Oh and Kim, 1990) and SKKU (Choi, 1987) to be utilized on several purposes including basis for setting up of a forecasting system at Central Meterological Office.

During the study of Abiki phenomena in Nagasaki Bay, Japanese Hydrographic Department (1981) also presented M_2 tidal model of the whole East China Sea of which the open bundary located along the Ryuku Islands arc (Fig. 14). French (LCHF) also developed a tidal model of the Yellow Sea adopting orthogonal curvilinear coordinate for evaluation of tidal modification of barriers in Inchon Bay but did not focus on reproduction of tides over the whole area due to large grid spacing.

During the last few years three-dimensional models of the East China Sea continental shelf and coastal area have been developed at KORDI and SKKU (Sung Kyun Kwan University) to compute vertical structure of currents induced by tide and meteorological forcing. As a first attempt, the deve-

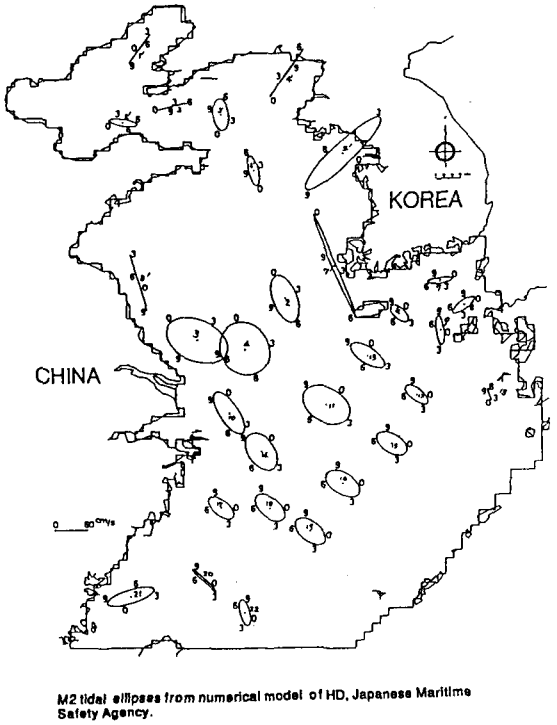

Fig. 14. M_2 tidal distribution from JHD model (JHD, 1981).

loped model was utilized to reproduce the three-dimensional current structure of the M_2, S_2, K_1 and O_1 tides (Choi, 1984a, 1985) representing the dominant tidal condition of the region. The computed results were used to provide maps of the tidal ellipses and tidal current constants at three depths. Current observations were performed along approximately 30 deg north latitude (Larsen *et al.*, 1985) and in the eastern Yellow Sea (Harkema and Hsueh, 1987). There was genenal agreement between the observations and three-dimensional tidal model of the area (Choi, 1984a; Choi, 1989). At the same time Fang, Yuan and Zhu (1989) also developed a three-dimensional model and applied to Bohai Sea.

3. GENERAL DESCRIPTION OF TIDES

3.1 Tides

The general tidal behaviour in the system may be conveniently presented by co-tidal lines and co-amplitude(co-range) lines of the empirical and model-derived charts described in previous section. The predominant feature is amphidromic regions located in the Gulfs of Bohai and Liaodong, off-Shandong Promontory and offshore region in the east coast of China. The existence of these amphidromic pionts may be explained by the ratio of the fundamental period of the system 46h, which is calculated by simple analytic model (Defant, 1961) and also from the model to that of tide generating force about 3.7 for the semi-diurnal tides and about 1.9 for the diurnal tides, thus having four amphidromes in the semi-diurnal tidal charts and two amphidromes in the diurnal charts.

There is a good qualitative agreement between the empirical and model-derived charts although,in the model, there is some deterioration in areas where the bottom topography is known to be complex and uncertain, particularly mid-Chinese coast where there is a large number of sand bars unresolved by the model. The amphidrom in the Liaodong Bay has been well reproduced by Chinese modelers. The model's disability to reproduce this point is due to use of large bottom friction. Fang and Yang (1985) mentioned that the distribution of tide in the Laizhou Bay, especially M_2 amphidromic point may have been changed due to the change of coastline of the Yellow River Delta. In Fig. 15 Ogura's old charts of M_2 and K_1 tides are shown and recent tidal charts due to coastal modification are presented in Fig. 16.

The K_1 cotidal chart is simpler than the M_2 chart and thus has less difference from historical K_1 chart than M_2. A relatively noticeable difference is that the present amphidromic piont in the Tsushima Strait is closer to the Korean coast (Odamaki, 1989, Fang and Yang, 1988a) than the historical one. From the charts, it is seen that both diurnal and semi-diurnal tides at the shelf edge propagate in a northwesterly direction to the entrance of the Yellow Sea (from Shanghai to the southern tip of Korea) as progressive waves. A part of tides entering across the shelf rotates counter-clockwise with its center at northern end of Taiwan (degenerate amphidromic points shown in M_2 tidal chart), counter-clockwise to southwest and progresses to Taiwan Strait. On entering the Yellow Sea, the tides progress to north along the west coast of Korea and after reaching the north shore of Yellow Sea, the tide turns its direction to west and progresses to Strait of Bohai. Then the tide progresses in a counter-clockwise direction along the coast in the Gulfs of Liaodong and Bohai and progresses to east along the south shore of the Bohai making a complete revolution within Gulfs of Liaodong and Bohai. The tides, after coming out from Bohai, progress down first to the southwest and then to the southeast along the coast of China. Thus the wave character in the Yellow Sea corresponds approximately to tide propagation in a rotating channel in the northern hemisphere described by Hendershott and Speranza (1971). Kang (1984) also presented an idea to explain the positioning of amphidromic points for the M_2 tide in the Yellow Sea by a superposition of Kelvin and Poincare waves. He explained that the large tidal range of Kyunggi Bay is due to the modifications of Poincare and Kelvin waves by Ongjin Peninsular.

Some features of the semidiurnal and diurnal tidal distribution are as follows:

Semi-diurnal tides:

(1) Maximum amplitudes of the M_2, S_2 elevations

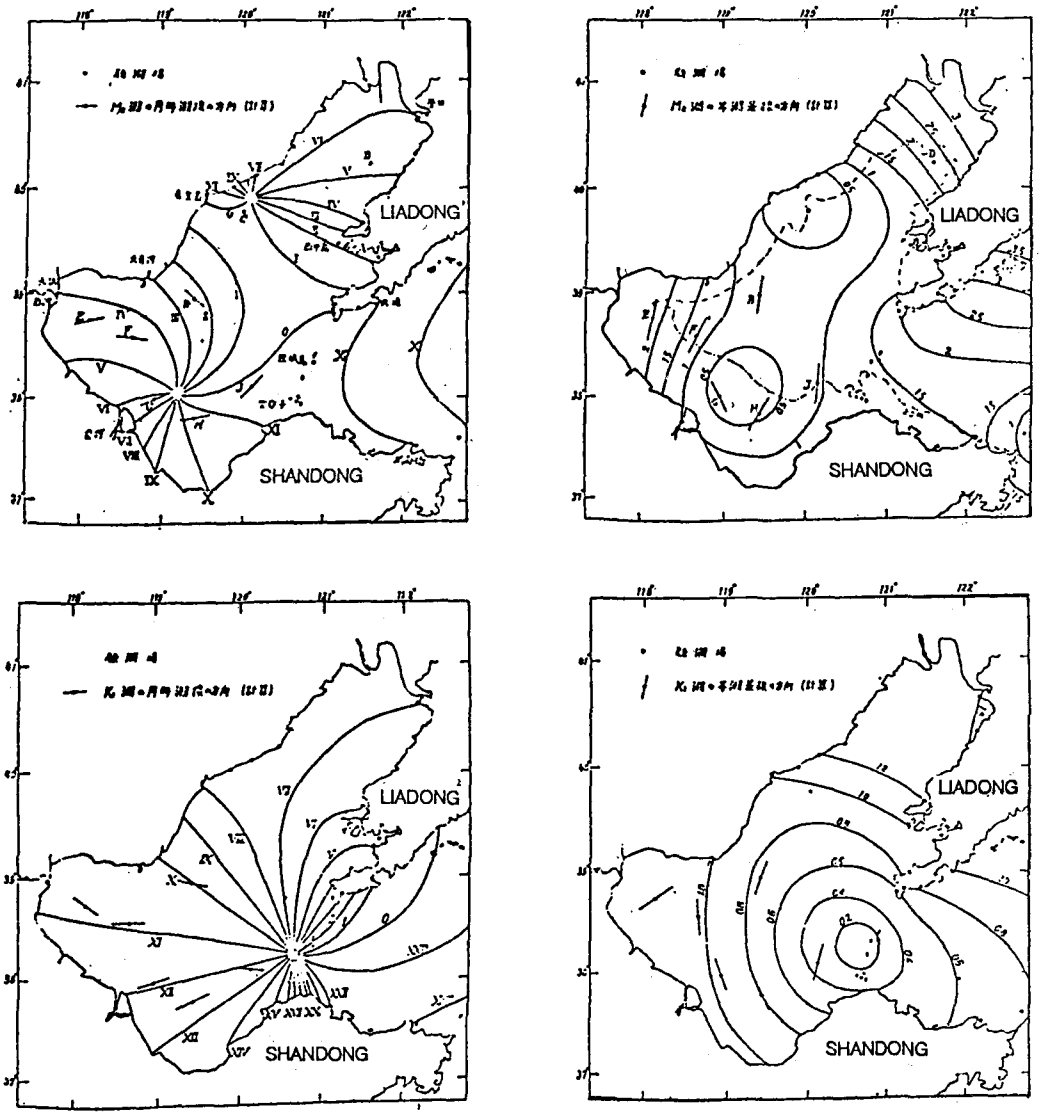

Fig. 15. M_2, K_1 tidal charts (Ogura, 1932).

are found at Inchon and Asan in Kyonggi Bay; especially 305 cm of M_2, 130 cm of S_2 amplitudes at Hwangsan do, located upper, inner part of Inchon Bay. The large semidiurnal tide in Kyonggi Bay is due to near-resonant oscillation (An, 1977; Choi, 1980; Kang, 1984).

(2) Both M_2 and S_2 tides progress very slowly in the southwest corner of Korea, and near the Changsan Promontory (38°N) off the west coast of Korea.

(3) A speculated position of amphidromic point in the southeast off Shandong Peninsula by Ogura at about latitude 35°N, longitude 121.5°E agrees well with the results of models. However, verification by direct measurement is still needed.

(4) Westward movement of an amphidromic point in Bohai (Laizhou) Bay compared to empirical charts is reproduced in the models (Dou *et al.*, 1981, Fang and Yang, 1985, Choi, 1989, Kang *et al.*, 1991).

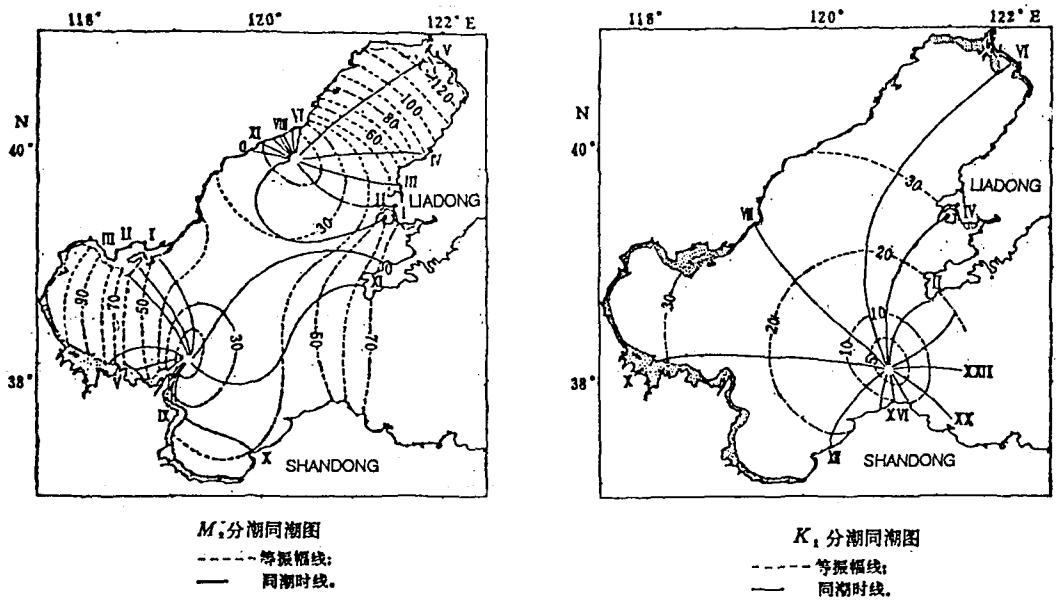

Fig. 16. M_2, K_1 tidal charts (Dou *et al.*, 1981).

Diurnal tides:

(1) Maximum amplitudes of the K_1, O_1 elevations are found at Unmu Island in Seohan Bay,

(2) Amplitudes of diurnal tides do not increase as much as those of semi-diurnal tides in Kyonggi Bay,

(3) The pattern of progress of diurnal tides in the Yellow Sea is similar to that of semi-diurnal tides but the change in velocity of the dirunal tides is greater over the shelf edge to entrance of the Yellow Sea and along the west coast of Korea.

3.2 Tidal currents

Fig. 17 shows the calculated M_2, S_2, K_1, and O_1 tidal ellipses (Choi, 1980) of selected points in the Yellow Sea and the Eastern China Sea. The ellipses charts give magnitude and direction of the tidal currents representing maximum and minimum velocity as major and minor axes, respectively and sense of rotation from 0 lunar hour (referenced to 135°E) is also indicated by arrows. These ellipses may give the overall picture of tidal current behaviour in the system.

Some feature of tidal currents in the system are as follows:

(1) The velocity of semi-diurnal currents is high at Jeju Strait (between southwest corner of Korea, and Jeju Island) and also along the west coast of Korea(south west corner of Korea, Kyonggi Bay, Seohan Bay) and the velocity at the entrance to the Changjiang and Qiantang Rivers and is of the order of 100 cm/sec. In many narrows between pensinsula and islands (Myongryang, Noryang, Gyunnaeryng) in the south coast of Korea, and between the Zhoushan Islands off central China west tidal currents exceed 3~4m/sec.

(2) The weakest semi-diurnal current with maximum M_2 speed smaller than 20 cm/sec is to be found along the south coast of Bohai Sea, off northern coast of the Shandong Peninsula and the in central Yellow Sea, besides south southeast East China Sea off continental slope. The semidiurnal current in the eastern entrance area of the Korea Strait is also weak (Fang, 1986).

(3) The regions of strong dirunal currents are similar to those of semi-diurnal currents where they are of the order of 40 cm/sec; other stronger diurnal currents computed are found to be at the narrows of the Kyushu Islands where they are of the order of 70 cm/sec and at Bohai Strait where they are about 40 cm/sec. Diurnal currents in the east and west channels of the Korea Strait are also relatively

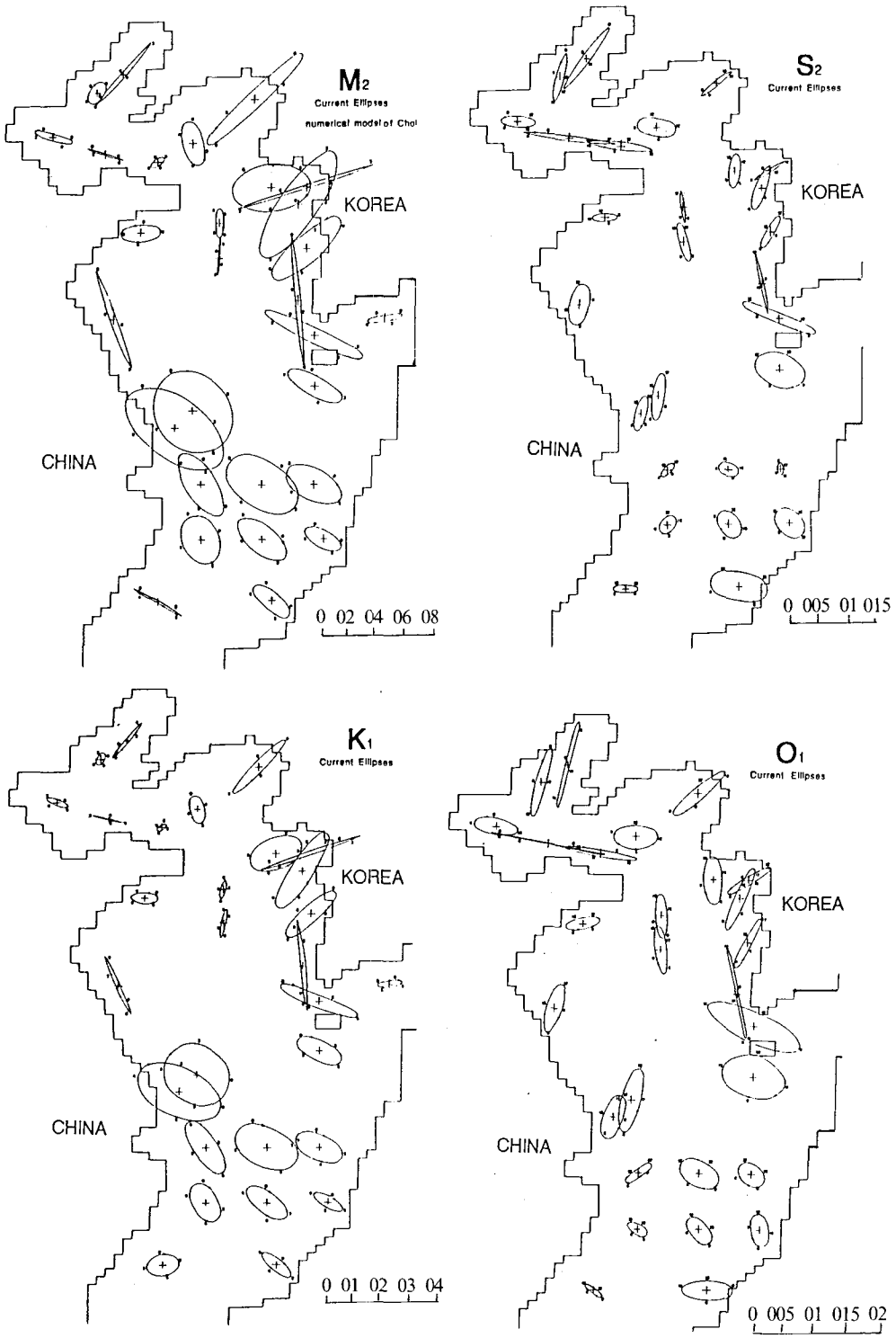

Fig. 17. Computed tidal ellipses of M_2, S_2, K_1, O_1 tides (Choi, 1980).

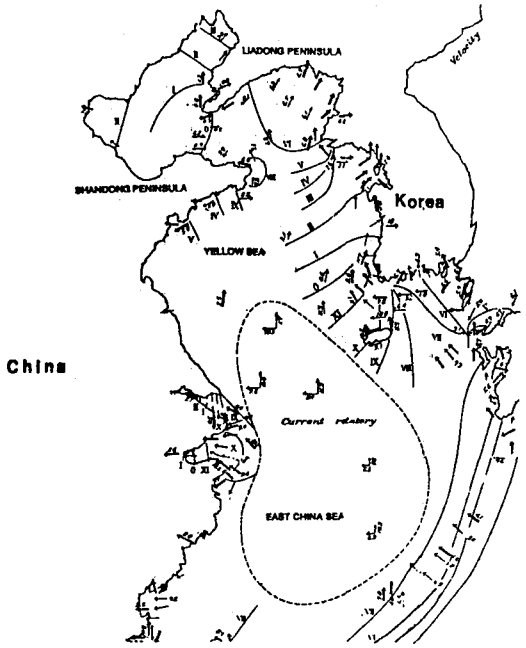

Fig. 18. Tidal current map of the East China Sea (Ogura, 1933).

strong,

(4) Generally speaking, tidal currents over the shelf from the continental edge to the entrance of the Yellow Sea are rotatory, in a clockwise direction through their periods, while the currents in the Yellow Sea are rectilinear following their direction of propagation along the coast.

Fig. 18 is a tidal current map presented by Ogura (1933a) and agrees well with the speculated rotary tidal current pattern over the East China Sea. Unlike the tidal amphidromic point, where the tide amplitude is zero, the velocity at current-amphidromic point is not usually zero. The character of tidal current at this point is that the current ellipse reduces to a circle and has no definite time of maximum velocity. Yet in the Eastern China Sea the M_2 currents at the current-amphidromic points are generally rather weak except for the point at the entrance of the Yellow Sea (Fang, 1986). Choi (1984 a) has also shown the computed tidal current distribution of M_2, S_2, K_1 and O_1 tides at three depth (Fig. 19). Saiki and Yanagino (1984) presented the tidal ellipses of the semi-diurnal current components in the sea to the west of Kyushou by statistically deducing from GEK data. Fang (1979) and Fang *et al.* (1991) presented theoretical explanation for the clockwise rotating current near the entrance of the Yellow Sea.

4. TIDAL DISSIPATION

Estimates of the rate of working of the Moon and Sun on the tides are generally at least twice the power loss of the tides in the shallow seas (Cartwright, 1978), and thus mark a serious unidentified sink of energy. Although an energy conversion to internal tides has been suggested as a large missing factor, present calculations have not yet balanced the energy budget.

As seen in Fig. 20 from Choi (1980), the energy dissipated by bottom friction of tidal current generally exceeds 500 erg/cm^2 where tidal currents are strong. At some localities it reaches about 1000 erg/cm^2. From model result, the rate of work at the shelf edge is 12.47×10^{10} W, which nearly balanced with the mean rate of frictional dissipation, 11.96×10^{10} W. The slight excess was due to the discrete nature of the numerical scheme used. Ding (1984) gives an estimate based on the numerical results by Fang and Yang (1985) of tidal energy flux accross the shelf edge to be 13.65×10^{10} W, which is quite close to Choi's result (1980).

The computed dissipation from the model (Choi, 1980) for the Yellow Sea and the East China Sea is about 7% of the total dissipation in the world's ocean comparing with 3% in the Bay of Fundy and Gulf of Main (Greenberg, 1979), and 11% in the Northwestern European shelf (Flather, 1976) with Miller's estimates of frictional dissipation of world's ocean 1.7×10^{12} W (Miller, 1966).

Based on the tidal constants at the two ends of mouth section and the variation of the ratio r (amplitude of neap tide to that of spring tide),from the mouth section to the closed end, the following results (for the Yellow Sea) have been obtained (Fang, 1979): (1) The energy flux of principal lunar and solar semidiurnal incident waves passing through the mouth section is 0.83×10^{18} erg/sec. (2) When the waves get to the closed end, about 46% (for

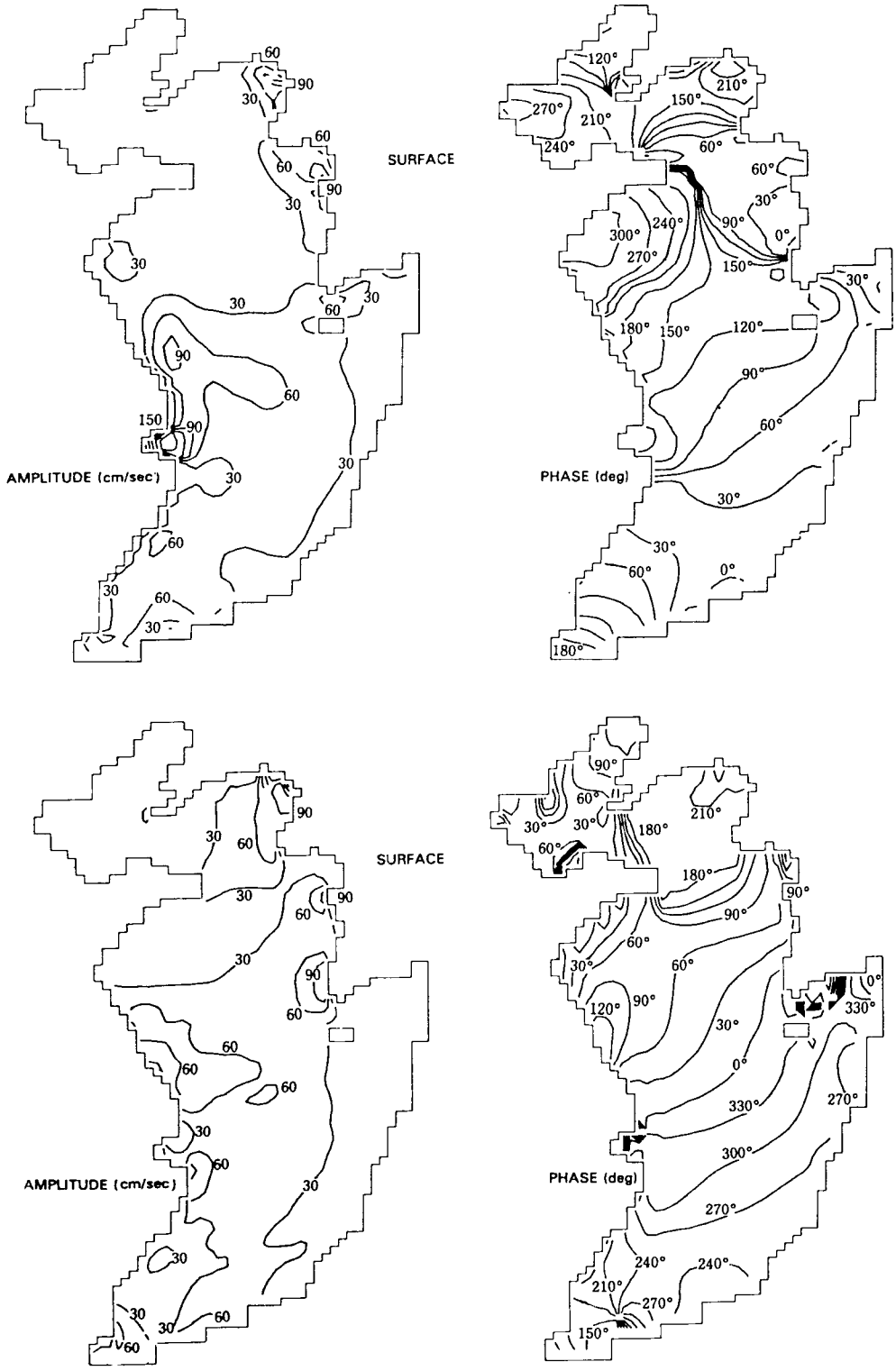

Fig. 19. Computed surface tidal current distribution from 3D model (Choi, 1984).

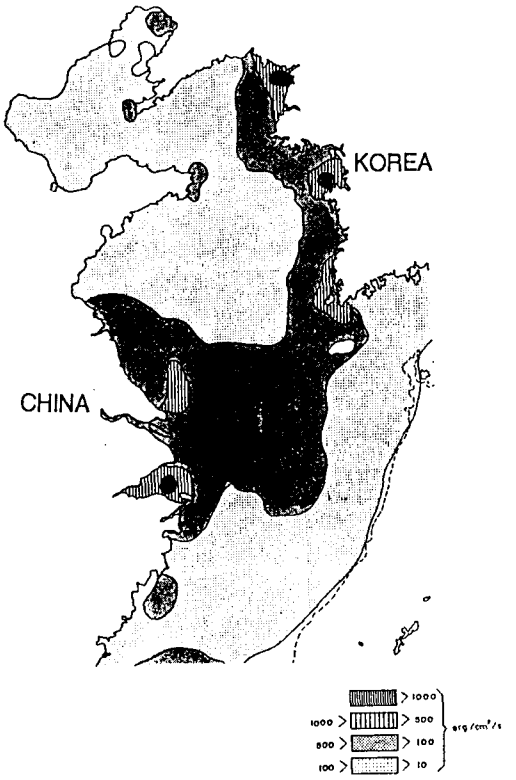

Fig. 20. Mean rate of bottom frictional energy dissipation from numerical model (Choi, 1980).

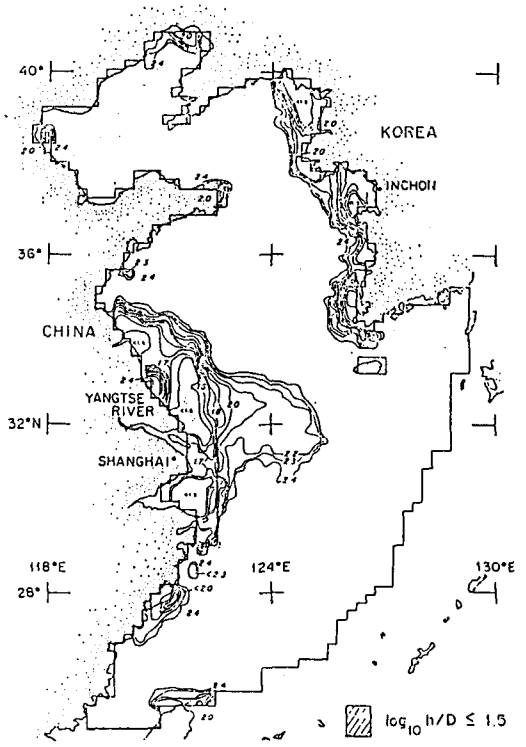

Fig. 21. Log(h/D) distribution in the East China Sea (Beardsley *et al.*, 1983).

neap tide) or 72% (for spring tide) of the energy has been dissipated. (3) The total energy of the principal lunar and solar semidiurnal tides in Hang Hai amounts to ca. 2.3×10^{23} erg. (4) The mean amplitude of tidal current is estimated to be about 49 cm/sec, and the mean range about 2.1m (5) The Q of semidiurnal tide is estimated to be 5.0 on the average (Fang, 1979). Choi (1980) estimated disspative Q as 6.0 for the whole East China Sea shelf based on model calculation. The computed results (Liu *et al.*, 1983) also showed that the tidal energy in the Bohai Sea is 0.91×10^{21} ergs and that in the Huanghai Sea 1.1×10^{22} ergs (Liu *et al.*, 1983). Zhou and Fang (1987) calculated coefficient of bottom friction in the Bohai Sea to be 0.0013. Fang *et al.* (1987) calculated the coefficient in the Hangzhou Bay using three methods and obtained the values ranging from 0.0005 to 0.00067. These are remarkably smaller than conventionally belived values. Fang also belives based on numerical experiments that 0.0015 is a suitable value for the Yellow Sea rather than 0.0032 which is derived from the nolineality of tidal friction bt Fang (1979).

5. TIDAL MIXING

Beardsley *et al.* (1983) used the predicted currents for the M_2 tide model (Choi, 1980) to estimate the influences of tidal mixing on the density structure of waters in the East China and Yellow Seas. They contour the parameter log (h/D), where h is the water depth and D the mean rate of the energy dissipation by the tides (Fig. 21). Values of this parameter <1.8 or 1.9 indicate a transition from well mixed (<1.8) to stratified (>1.9). Regions where mixing should dominate based upon these criteria are the west coast of Korea and the region surrounding the mouth of the Changjiang. The model does hold

for the Korean coast however near the Changjiang the input of buoyancy from the fresh river waters is too great to allow mixing to destratify the system. However in this region the lower layers of the water column, 20 to 35m, are well mixed and estimates of the Richardson number indicated near neutral stability.

Tidal mixing fronts in the eastern Yellow Sea are even more prominent at some localities, such as near the promontory of Tae An Peninsula and around some islands off the south western tip of Korea. The resulting horizontal distribution of temperature in the summer time is cold coastal and warm offshore water at the surface but warm coastal and cold offshore water below the thermocline depth. In the central part of the basin, the thermocline lies 10-20m below the surface with vertical temperature gradient greater than 1℃. Extensive measurements around the tidal mixing front near the promontory of Tae An Peninsula show that the front begins to appear in April with the start of solar heating, becomes most clear in August and disappears in November with the start of surface cooling. KORDI also performed comprehensive CTD survey in southeastern Yellow Sea and reported tidal front structure there (Lie, 1989).

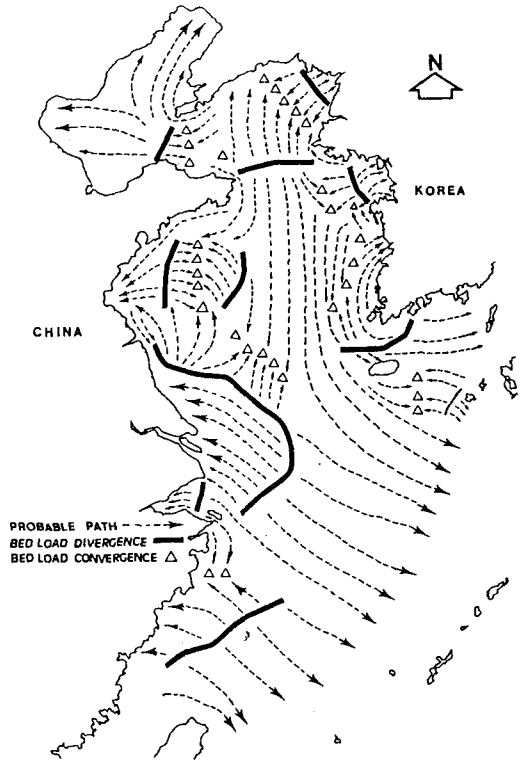

Fig. 22. Probable sediment transport paths (Choi, 1986).

6. TIDAL SEDIMENTATION

Dynamic tidal sedimentation in the region is also of a continuing research interest. The prediction of the local and regional sand transport directions of the offshore tidal sand banks in the shelf has been performed on the basis of diagrammatical method. There was general agreement with these predictions and the earlier prediction (Choi, 1983) of net regional sand transport paths from the numerical simulation of the maximum bottom stress vectors during the semi-diurnal period due to the M_2 and M_4 tides from the shelf model. A map of probable sediment transport paths in the shelf was presented as shown Fig. 22. Milliman *et al.* (1985) also utilized the bottom stress field from the shelf model to study transport mechanism of modern accumulation of sediment on the shelf (Fig. 23). Sternberg *et al.* (1983) estimated that the critical bottom stress needed to initiate sediment movement is approximately 2.0 to 2.0 dyn cm^{-2} in those region. Since the maximum bottom stress associated with the M_2 and M_4 tidal currents exceeds this threshold value by at least a factor of 2 over much of the East China Sea, tidal currents must play an important role in the regional sediment dynamics. This information about sand of sea floor swept by strong tidal currents as well as deposits formed by them are of practical importance from the viewpoints of safety of shipping and underwater line structures.

7. TIDAL CIRCULATION

Fig. 24 and Fig. 25 repectively show the computed large scale feature of tidal circulation obtained from the models (Choi, 1990; Tang, 1990). Relatively strong residual current were calculated along the coast of Korea and China, around Jeju Island. Strong eddies were also formed in the Seohan Bay,

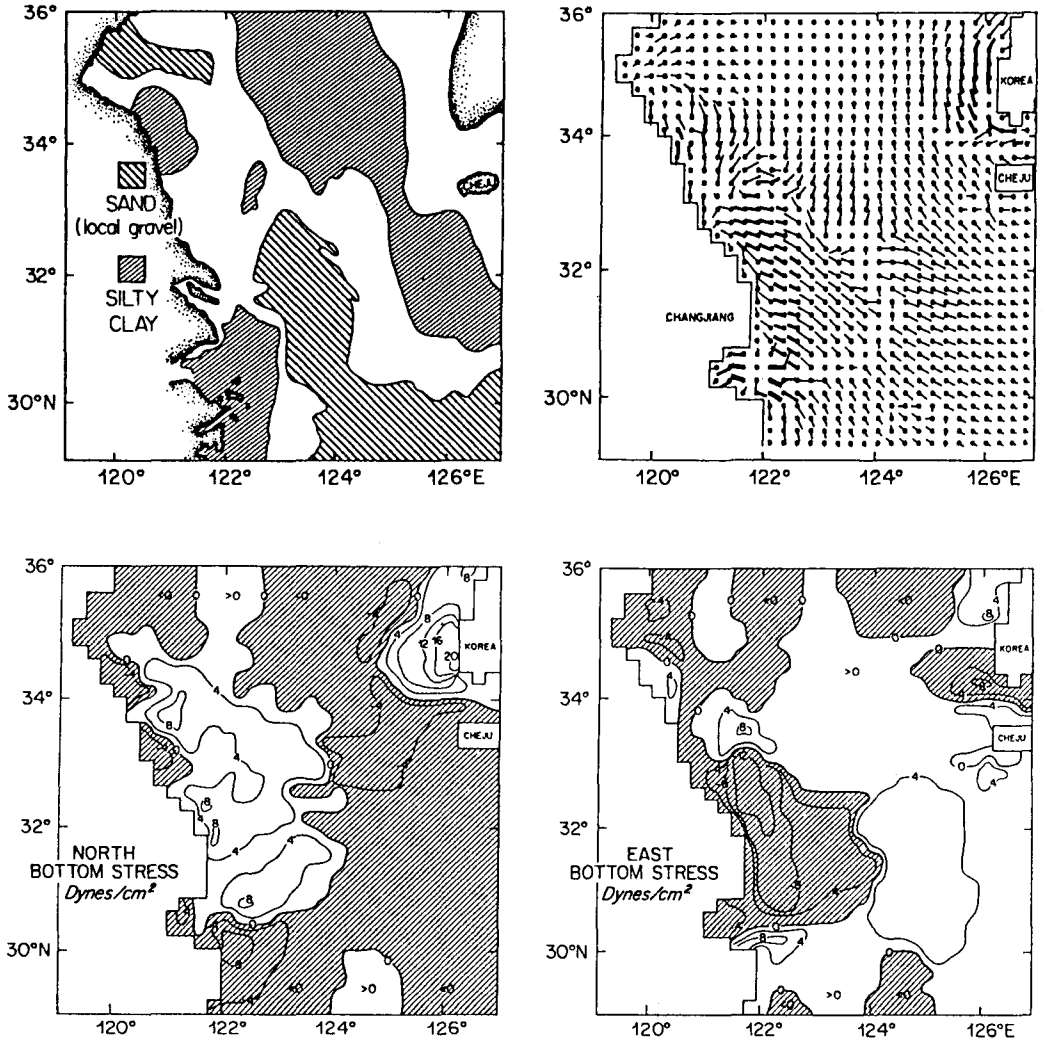

Fig. 23. Comparison of maximum bottom stress vectors and distribution of sediment in the Yellow Sea (Milliman *et al.*, 1985).

Kyonggi Bay and over shallow bank area at Chinese coasts. Current data in the region are scarce to verify the model derived tidal circulation. Tidal residual circulation in central Yellow Sea is weak and baroclinic current associated with cold water mass may be significantly greater than tidal residual. However distinctive trajectories from satellite tracked drifters (Fig. 26) showed that a drifter deployed at mid Yellow Sea late July 1987 moved slowly with counterclockwise sense during two month period. This striking feature is at first reasonably well reproduced by model with very weak residual currents in the region. Another drifter displayed off the mouth of the Changjiang River about same period moved 600 km in two months with an averaged speed of 11.6 cm/sec toward the Cheju Strait and the western channel of Korea to enter the East Sea(Japan Sea). These tracks are consistent with the movement of the Changjiang diluted water aside from pure contribution of tidal circulation (Kim, 1988).

8. CONCLUDING REMARKS

Sources of errors of the numerical tidal model

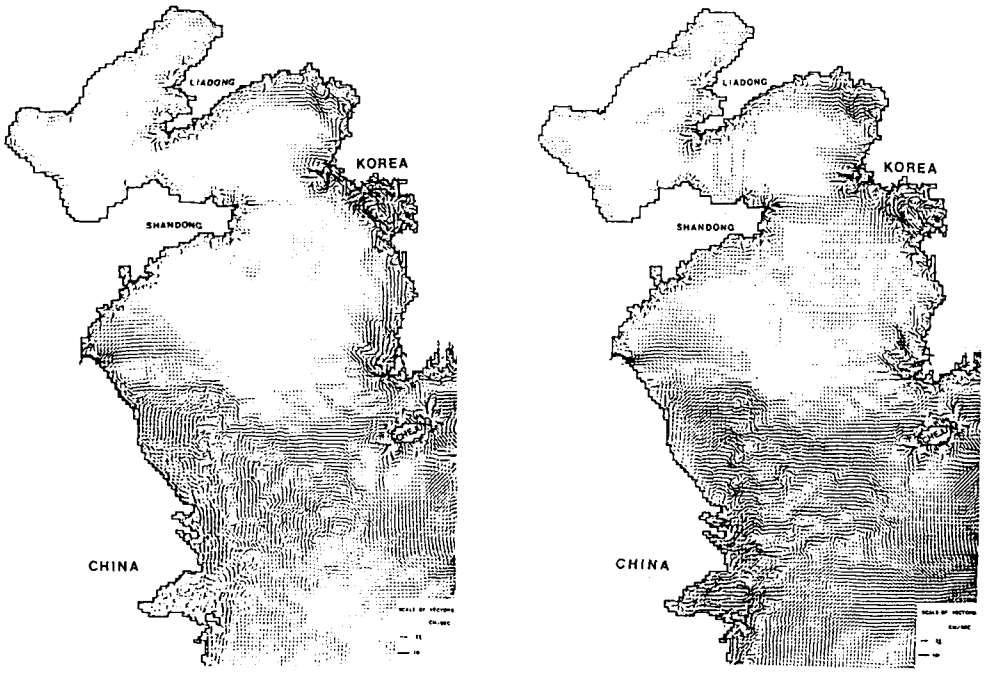

Eulerian residual current from the two-dimensional model.

First-order Lagrangian residual current from the two-dimensional model.

Fig. 24. Computed tidal residual currents in the Yellow Sea (Choi, 1990).

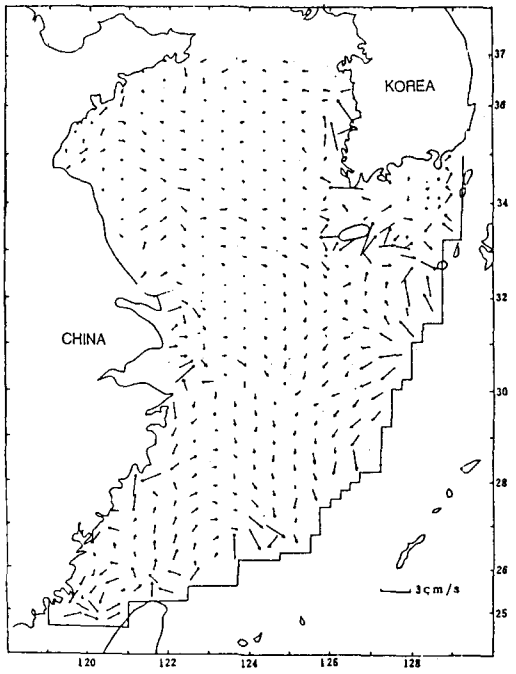

Fig. 25. Computed tidal residual currents in the Yellow Sea (Tang, 1990).

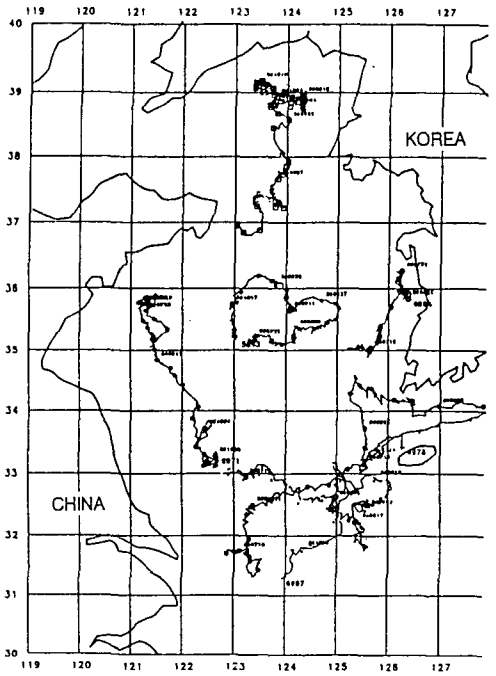

Fig. 26. Track of ARGOS satellite drifter buoys during Jul.-Oct., 1986.

are dynamical approxmation, topographic error in numerical finite difference scheme, interpolating error fundamental dependence of the model solution upon the unreliable data spècifed on the open boundary. Probable limitation of depth-integrated numerical model is that phase calculated model tends to lag resulting over-estimation of phase. The numerical computation by means of boundary value method usually can not give good results for open sea, and that by means of initial value method sometimes does not agree with the observed data satisfactorily (Fang, 1986).

At present capability of numerical ocean circulation models have not reached at operational predictive stage mainly because of insufficient boundary observations at continental shelf edge, long-term current observation and real-time temperature and salinity data. However, initial settings to investigate the tidal physics and associtated dynamic problems in the Yellow Sea and the East China Sea, based on dynamic principles, appear to have been laid. Models limiting to coastal and estuarine area are widely practised to evaluate environmental changes due to coastal development including new port, artificial islands and large land reclamation projects of the region. Necessites of accurate tidal prediction over the whole region in terms of tidal elevation and vertical structure of tidal current are increasing due to wide utilization of ADCPs in the region and launching of TOPEX/POSEIDON satellite. In order to utilize the vertical current profile from the ADCPs and the altimeter measurements in circulation studies, it is important that the tidal signal be removed via accurate tidal predictions from the model or proper alternative way.

ACKNOWLEDGEMENTS

This review was prepared during the course of a cooperative work in Korea-China Yellow Sea Resource Development study (Ocean Atlas work) and presented at 7th JECSS Workshop, helded in Qingdao, 1993. Thanks are due to Ministry of Science and Technology for providing financial support through Prof. Young Chul Lee (Inha University), Principal Investigator of the Project.

REFERENCES

An, H.S., 1977. A numerical experiment of the M_2 tide in the Yellow sea, *Journal of the Oceanographical Society of Japan*, **33**, pp. 103-110.

Beardsley, R.C., Limeburner, R., Dunxin Hu, Cannon, G.A. and Pashinski, D.J., 1983. Structure of the Changjiang River plume in the East China Sea during June, 1980, International Symposium on the Sedimention on the Continental Shelf, with special reference to the East China Sea, China Ocean Press, pp. 265-284.

Boris, L.I., 1958. Calculation of the tides and tidal currents in the Yellow Sea, Trudy Leningrad Gridromet Inst. Report No. 7. (in Russian).

Cao, D. and Fang, G., 1985. A numerical computation of the tides and tidal currents in the Bay of Hangzhou, (*Oceanologia et Limnologia Sinica*, in Chinese, English abstract).

Cartwright, D.E., 1978. Oceanic tides, *Intertional Hydrographic Review*, Vol LX(2), 35-84.

Choi, B.H., 1980. A tidal model of the Yellow Sea and the Eastern China Sea, Korea Ocean Reserch and Development Institute Report 80-02.

Choi, B.H., 1983. Sediment transport paths in the East Chins Sea, *Jornal of the Korean Society of Civil Engineers*, **3**(4): pp. 83-93. (in Korean, English abstract).

Choi, B.H., 1984a. A three-dimensional model of the East China Sea, In, pp. Ocean Hydrodynamics of the Japan and East China Seas, T. Ichiye, editor, Elsevier Oceanography Series 39, pp. 209-224.

Choi, B.H., 1984b. A stratification/mixing model of the yellow sea and the East China Sea, *Journal of the Korea Society of Civil Engineers*, **4**(2): pp. 125-132. (in Korean, English abstract).

Choi, B.H., 1985. Observed and computed tidal currents in the East China Sea, *Journal of the Oceanological Society of Korea*, **20**(1): pp. 56-73.

Choi, B.H., 1986. Tidal computation for the Yellow Sea, Abstract of paper presented at 20th I.C.C.E., Taiwan, 9-14 November, pp. 67-81.

Choi, B.H., 1987. Development of tide and surge models of the Yellow Sea for coastal engineering application, Proceedings of 2nd conferrence on coastal and port engineering in developing countries, Beijing, China, pp. 1880-1894.

Choi, B.H., 1989. A fine-grid three-dimensional M_2 todal model of the East China Sea, In Modeling Marine System, (ed.) Davies, A.M. , CRC publications.

Choi, B.H., Predictions of sand transport directions of the offshore tidal sand banks in the Yellow Sea, Proc. 5th Cong. APD, Int. Assoc. Hydraulic Res., 1986, 231.

Choi, B.H., 1990. Deveopment of fine-grid mumerical tidal models of the Yellow Sea and the East China Sea, *Journal of Korea Society of Coastal and Ocean Engineers*, **2**(4): pp. 231-234. (in Korean English abstract).

Defant, A., 1961. Physical oceanography, Oxford, Pergamon Press.

Ding, W., 1983. The characteristic of the tides and tidal